




A novel acid polysaccharide from *Boletus edulis*: extraction, characteristics and antitumor activities *in vitro*

Ting Meng^{1,2} · Sha-sha Yu^{1,2} · Hai-yu Ji^{1,2,3} · Xiao-meng Xu^{1,2} · An-jun Liu^{1,2} 

Received: 5 October 2020 / Revised: 1 December 2020 / Accepted: 3 January 2021 / Published online: 28 January 2021
© The Author(s), under exclusive licence to Springer Science+Business Media, LLC part of Springer Nature 2021

Abstract

A novel cold-water-soluble polysaccharide (BEP), with a molecular weight of 6.0×10^6 Da, was isolated from *Boletus edulis*. BEP consists of galactose, glucose, xylose, mannose, glucuronic, and galacturonic acid in a ratio of 0.34:0.28:0.28:2.57:1.00:0.44. The IR results showed that BEP was an acid polysaccharide, containing α -type and β -type glucoside bonds. MTT assay showed BEP could inhibit cell proliferation significantly. Morphological observation demonstrated that BEP-treated MDA-MB-231 and Ca761 cells exhibited typical apoptotic morphological features. Flow cytometry analysis revealed that BEP caused mitochondrial membrane potential collapse. Annexin V-FITC/PI staining indicated that BEP induced apoptosis of MDA-MB-231 and Ca761 cells through cell block in S phase and G₀/G₁ phase, respectively. Western blot results showed that BEP could increase the Bax/Bcl-2 ratios, promote the release of cytochrome C, and activate the expression of caspase-3 and caspase-9 in MDA-MB-231 and Ca761 cells. In conclusion, our results demonstrated that BEP could inhibit the proliferation of breast cancer cells and induce apoptosis through mitochondrial pathways.

Keywords *Boletus edulis* · Breast cancer · Cell apoptosis · Mitochondrial pathway

Introduction

Breast cancer is one of the most common cancers among women in the world, and its incidence is increasing year by year [1, 2]. Since 2013, breast cancers have been divided into four different subgroups by molecular characterize, which determine the imparity recommended standard treatments and the patient's prognosis [3]. Because triple-negative breast cancer (TNBC) lacks the expression of three common tumor markers, estrogen receptor (ER), progesterone receptor (PR), and human epidermal growth factor receptor 2 (HER2), so it appears to be more aggressive than the other breast cancer subtypes [4]. TNBC is also often characterized by younger age, higher rates of “spaced” breast cancer (detected between

screenings), and adverse features such as cell necrosis and high mitotic index [5–7]. TNBC is resistant to the usual treatment of breast cancer, such as endocrine therapy, and is prone to metastasis and recurrence [8]. Therefore, it is necessary to find new natural anti-tumor active substances to reduce side effects. Studies have shown that polysaccharide HPA extracted from the marine fungus *Hansfordia sinousae* can inhibit the proliferation of HeLa and MCF-7 cells and induce cell apoptosis through mitochondrial apoptosis [9].

Apoptosis, also known as programmed cell death, is crucial for normal tissue development [10]. Abnormalities in this pathway can lead to various diseases and even cancer [11]. Most of the chemotherapeutic agents kill cancer cells by inhibiting their proliferation and inducing their apoptosis pathways [12]. During apoptosis, some typical apoptotic characteristics occur in cells, such as vesiculation, cell contraction, the formation of apoptotic bodies, condensation chromatin, DNA fragmentation, and activation of cysteinyl aspartate-specific proteinases: the caspases [13]. The apoptotic pathway can be divided into extrinsic and intrinsic apoptotic pathways [14]. The activation of the intrinsic apoptotic pathway plays a role through mitochondria, which is the center of the apoptosis pathway [15]. The mitochondrial apoptosis pathway starts from mitochondrial depolarization, which is regulated by

✉ An-jun Liu
15222017003@163.com

¹ State Key Laboratory of Food Nutrition and Safety, Tianjin University of Science and Technology, No. 29, 13th street, TEDA, Tianjin 300457, People's Republic of China

² College of Food Science and Engineering, Tianjin University of Science and Technology, Tianjin 300457, China

³ QingYunTang Biotech (Beijing) Co., Ltd., Beijing 100176, China

members of the Bcl-2 protein family, leads to the release of cytochrome c, thereby activates caspase-9 and caspase-3, ultimately leads to apoptosis, forming the apoptosome [16, 17].

Mushrooms have been consumed for centuries because they are a good source of valuable nutraceuticals and medicines, which are rich in protein, polysaccharides, dietary fibers, essential minerals, and secondary metabolites [18, 19]. The main components of mushroom bioactivity are polysaccharides and polysaccharide-protein complexes. Some of these compounds have good anti-tumor, anti-inflammatory, and antioxidant activities that can regulate the immune system [20], such as the bioactive ingredients extracted from *Ganoderma lucidum* [9]. *Boletus edulis* (*Boletus edulis* Bull. Fr.), also known as “king bolete”, is a kind of edible wild-growing mushroom that is very popular around the world [21]. The modern pharmacological studies show that it has anti-diabetes, antioxidant and anti-tumor activity [22]. At present, most studies on polysaccharides from *Boletus edulis* concentrate on the optimization of extraction conditions [23], structure analysis [24], and anti-oxidation [25], while there are few studies on its anti-tumor [26, 27]. Moreover, the extraction method is mostly traditional hot water extraction, and the obtained polysaccharides are neutral polysaccharides with small molecular weight. Therefore, the extraction of new active polysaccharides from *Boletus edulis* and the study of its anti-tumor mechanism provides a theoretical foundation for its practical application in the future. In this study, a novel water-soluble polysaccharide from *Boletus edulis* (BEP) was extracted and purified at 4 °C, and its preliminary structure and anti-tumor activity in MDA-MB-231 and Ca761 cells were studied.

Materials and methods

Reagents and chemicals

Dried fruiting bodies of *Boletus edulis* were purchased from Lingyutang Group Co. Ltd. (Yunnan, China). D-glucose (Glc), L-rhamnose (Rha), L-arabinose (Ara), D-mannose (Man), D-galactose (Gal), D-xylose (Xyl), D-glucuronic acid (GlcA), D-galacturonic (GalA) and trifluoroacetic acid (TFA) were purchased from Solarbio Science & Technology Co., Ltd. (Beijing, China). RPMI-1640 Medium was provided by GIBCO (Carlsbad, CA, USA). MTT and DMSO were provided by Sigma Chemical Co. (St. Louis, MO, USA). Annexin V-FITC/PI apoptosis detection kit was purchased from Keygen Biotech (Nanjing, China). Hoechst 33258, Hoechst 33342/PI double-staining, Bradford protein assay (BCA), Rhodamine 123, ROS assay kits, PMSF, and ECL kit were obtained from Solarbio Science & Technology Co. Ltd. (Beijing, China). The antibodies specific to β -actin, Bcl-2, Bax, caspase-9, caspase-3, and cytochrome C were provided

from Beyotime Institute of Biotechnology (Shanghai, China). All other chemical reagents were of analytical grade.

Extraction, separation and purification of BEP

The dried *Boletus edulis* were shattered to powder and then extracted by cold water method (liquid-solid ratio of 15:1, extraction temperature of 4 °C, extraction time of 7 h). The extracting solution was then precipitated with ethanol at a concentration of 60%. The protein was removed by sewage method [28], and small molecular impurities were removed by dialysis with 100,000 dialysis bags to obtain pure BEP polysaccharide.

Chemical components of BEP

Total sugar content and protein content in BEP were determined by the phenol sulfuric acid method (glucose as standard) and Coomassie bright blue method (bovine serum protein as standard) [29–31]. The contents of protein and nucleic acid [32] in BEP were detected by the UV-2550 spectrophotometer between 200 and 800 nm (CARY 50 UV-Vis, Agilent).

Determination of homogeneity and molecular weight

The homogeneity and molecular weight of BEP were determined by HPLC (HPGPC, Agilent-1200, USA) equipped with TSK-GEL G4000PW_{XL} (7.8 mm × 300 mm), a refractive index detector. The linear regression was calibrated with T-series standards (T10, T40, T70, T110, T500, T2000) [24]. The sample was dissolved to a concentration of 1 mg/mL by distilled water, and 20 μ L of supernatant was injected for each run and eluted with ultrapure water at a flow rate of 0.8 mL/min at 35 °C. [33].

FT-IR spectrum analysis

Weigh 1 mg sample, 150 mg dried potassium bromide powder, ground them fully until they were attached to the wall, then put them into the mold for tablet pressing (pressurized to 8 t, lasting 30 s). After collecting the background, the FT-IR spectrum (KBr pellets) of the polysaccharide sample was collected in the wavelength range of 4000–400 cm^{-1} on the FT-IR (Bruker VECTOR-220, German) [34].

Monosaccharide composition analysis

The monosaccharide compositions of BEP were detected by the IC (Ion Chromatography) on a Dionex ICS5000 chromatographic system, with a Dionex pulsed amperometric detector with an Au electrode and an efficient anion exchange column of Dionex CarboPac PA10 column (250 mm ×

2.0 mm) [35]. 10 mg BEP was hydrolyzed with 2 mL of 2 M TFA and degraded in an oil bath at 110 °C for 3 h. After that, adding 1 mL of methanol and also dried with N₂, and repeated 3 times. Finally, the degraded blow-dried polysaccharides were dissolved in ultra-pure water and diluted to a final concentration of 50 ppm for IC analysis. D-rhamnose, L-arabinose, D-galactose, D-glucose, L-xylose, D-mannose, D-glucuronic acid, and D-galacturonic acid were applied as standards.

Cell culture

The human breast cancer MDA-MB-231 and mouse breast cancer Ca761 cell line (Tianjin Medical University, Tianjin, China) were cultured in RPMI-1640 containing 10% heat-inactivated fetal bovine serum. The cells were cultured in a humidified incubator containing 5% CO₂ at 37 °C. All experimental cells were performed by passage 5–10 times after MDA-MB-231 and Ca761 cells had grown to exponential growth stage.

MTT assay

The MDA-MB-231 and Ca761 cells viability were evaluated by MTT assay. When the cells were in the logarithmic growth stage, the MDA-MB-231 and Ca761 cells were cultured in 96-well plates with the final concentration of 5×10^3 cells/well. After the cells adhered to the plate wells, different concentrations of BEP (25, 50, 75, 100, 125, 150, 200, 400, 600 µg/mL) were added and cultured by incubation for 24 h and 48 h at 37 °C in a 5% CO₂ incubator, respectively. Then, 20 µL MTT solution (5 mg/mL) was added to each well, followed by incubation for another 4 h at 37 °C. After the supernatant was removed, 150 µL DMSO was added to dissolve the crystals. The absorbance of the solution at 570 nm was detected by a microplate reader (Model 680, Bio-Rad, Hercules, CA, USA). The cell growth inhibition rate was calculated as follows:

Inhibition rate (%)

$$= (\text{untreated groups} - \text{experimental groups}) / \text{untreated groups} \times 100$$

Cell morphology observation

Observed under an inverted fluorescence microscope

When the cells reached the logarithmic growth stage, they were treated with different concentrations of BEP (0, 75, 150, 300 µg/mL) and cultured in a humidified incubator containing 5% CO₂ at 37 °C for 24 h before being photographed

under an inverted fluorescence microscope. (Nikon, Tokyo, Japan).

Hoechst 33258 staining

Hoechst 33258 staining was used to observe the morphological changes of the apoptotic cell nucleus [36]. The treated cells were washed twice with PBS buffer, fixed with paraformaldehyde (4%) for 15 min. Next, the cells were stained with Hoechst 33258 of 10 µg/mL for 20 min at room temperature. Finally, the stained nuclei were observed with an inverted fluorescence microscope (Nikon ECLIPSE 90i, Tokyo, Japan).

Hoechst 33342/PI double staining

The treated cells with BEP for 24 h were fixed with 4% formaldehyde, then stained with Hoechst 33342 and PI for 20 min, and finally, the cell morphology was observed [36].

Cell apoptosis assay

The cell apoptosis rates were determined by Annexin V-FITC/PI staining. According to the manufacturer's instructions, the control and experimental cells were collected and resuspended in 500 µL 1 × Binding Buffer, followed by 5 µL Annexin V-FITC and 5 µL PI, which were incubated for 10 min at 37 °C in the dark. Finally, the apoptosis rate of the stained cells was determined by flow cytometry within 1 h.

Mitochondrial membrane potential ($\Delta\Psi_m$) analysis

The cationic fluorescent dye rhodamine 123 was used to detect mitochondrial membrane potential changes in MDA-MB-231 and Ca761 cells treated with different concentrations of BEP for 24 h. According to the manufacturer's instructions, the cells were collected and stained with rhodamine 123 dye (10 µg/mL) at 37 °C for 30 min in the dark. Finally, the cells were washed with PBS for 3 times, resuspended with 500 µL PBS and detected by flow cytometry.

Measurement of intracellular ROS generation

Changes in DCFH-DA fluorescence intensity can be used to quantitatively detect intracellular reactive oxygen species. According to the ROS detection kit, the cells were harvested and washed with PBS. After that, the cells were resuspended with 1 mL PBS containing DCFH-DA (10 µM) and incubated at 37 °C for 20 min in the dark. Finally, after the residual DCFH-DA was washed with PBS, the cells were detected by flow cytometry.

Cell cycle analysis

The control and treated cells were collected and resuspended with 1 mL PBS, added to 70% ethanol drop by drop, and fixed overnight at 4 °C. Finally, the fixed cells were washed and incubated with 50 µL RNase A (1 mg/mL) at 37 °C for 30 min, and stained with 50 µL PI (0.5 µg/mL) at 4 °C for 10 min in the dark. The proportion of cells in each phase were detected by flow cytometry.

Western blotting

Western blotting was used to detect the expression of apoptosis-related proteins in MDA-MB-231 and Ca761 cells after BEP treatment for 24 h. The cells were digested with trypsin, washed with PBS for three times, and lysed on ice with RIPA lysate containing PMSF for 30 min, followed by centrifugation (12,000 g for 8 min) at 4 °C. Bradford protein assay kit was used to quantify the obtained proteins. After that, the proteins were mixed with 2× loading buffer and boiled for 5 min. Protein samples were separated with 12% SDS-PAGE and transferred to PVDF membrane by the Trans-Blot SD Semi-Dry Transfer Cell (BIO-RAD). The membrane was blocked with 5% BSA at room temperature for 2 h and then incubated with the corresponding primary antibodies (anti-β-actin, anti-Bax, anti-Bcl-2, anti-cytochrome C, anti-caspase-3, and anti-caspase-9) overnight at 4 °C. The membranes were washed with TBST for 3 times (15 min each time) and incubated with the corresponding horseradish peroxidase-labeled secondary antibodies at room temperature for 1.5 h. The protein bands were detected with the ECL assay kit and exposed to an X-ray in a darkroom.

Statistical analysis

All experiments were performed at least three times, and all the data were presented as mean ± standard deviation. One-way analysis of variance and Student's *t* test were used to analyze the statistical significance of the results. $P < 0.05$ was considered to be significant.

Results and discussion

Chemical compositions

The sugar contents and uronic acid contents of BEP extracted by 60% alcohol precipitation at 4 °C were 92.20% and 12.62%, respectively. As shown in Fig. 1e, there was a weak absorption peak at 260 nm and 280 nm by UV-vis spectrophotometer, indicating that BEP contains a trace of proteins and nucleic acids.

Molecular weights of BEP

The HPGPC showed that the BEP presented a symmetrical and narrow peak (Fig. 1c). According to the standard curve: $y = -0.5416x + 10.363$, $R^2 = 0.9944$, the average molecular weight of BEP was 6.0×10^6 Da.

Analysis of FT-IR spectral characteristics

The FT-IR spectra of BEP were shown in Fig. 1d. The strong absorption peaks at 3397.31 cm^{-1} and 2926.10 cm^{-1} were respectively the characteristic stretching vibration peaks of the hydroxyl group and C-H on the polysaccharides. The absorption peaks at 1643.69 cm^{-1} and 1412.56 cm^{-1} are generated by the stretching vibration of carbonyl in the functional group -COOH, indicating that BEP may contain uronic acid. The absorption peaks at 1135.91 cm^{-1} and 1053.15 cm^{-1} showed that the presence of pyranose ring in BEP [37]. Besides, the absorption at 917.25 cm^{-1} and 826.96 cm^{-1} indicated that the β-glycosidic bond and α-glycosidic bond existed in BEP [38].

The monosaccharide composition

IC results (Fig. 1a, b) showed that BEP was mainly composed of mannose, glucuronic and galacturonic acid, and contained a small amount of galactose, glucose and xylose in a ratio of 2.57:1.00:0.44:0.34:0.28:0.28, indicating that BEP was an acidic polysaccharide, which is consistent with the results of IR.

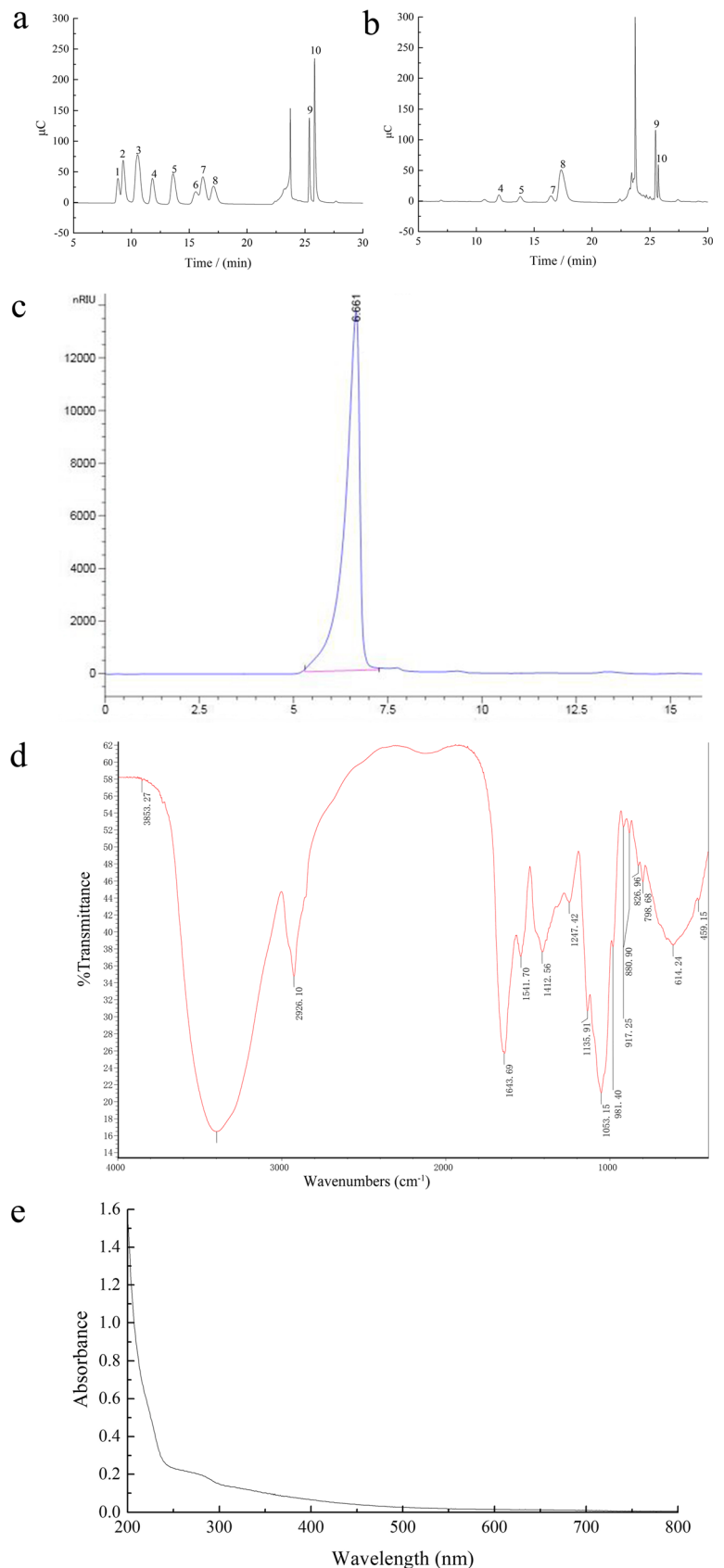
Inhibitory effect of BEP on breast cancer cells

MTT assay was used to detect the proliferation inhibition effect of BEP on MDA-MB-231 and Ca761 cells after exposed for 24 h and 48 h. As shown in Fig. 2a, BEP significantly inhibited the proliferation of MDA-MB-231 and Ca761 cells in a dose-dependent manner. The inhibition rate of BEP under 75 µg/mL on MDA-MB-231 and Ca761 cells were less than 30%, and the inhibition effect was not evident. After treatment of BEP on MDA-MB-231 and Ca761 cells, the IC₅₀ values were 152.76 µg/mL and 134.55 µg/mL for 24 h, were 120.62 µg/mL and 105.37 µg/mL for 48 h, which indicated that Ca761 cells were more sensitive to BEP. Therefore, the concentration of 0, 75, 150 and 300 µg/mL of BEP were selected in the following experiments.

Cell morphological observation

As shown in Fig. 3a, d, the untreated MDA-MB-231 and Ca761 cells had smooth surfaces, clear edges and normal shape. However, after BEP treatment, the morphology of MDA-MB-231 and Ca761 cells changed significantly, the

Fig. 1 Ion chromatography (Dionex pulsed amperometric detector) analysis of the standard monosaccharides (**a**) and BEP (**b**): (1) rhamnose (Rha); (2) arabinose (Ara); (3) glucosamine (GlcN); (4) galactose (Gal); (5) glucose (Glc); (6) acetylglucosamine (GlcNAc); (7) xylose (Xyl); (8) mannose (Man); (9) glucuronic acid; (10) galacturonic acid; the big peak between peaks 8 and 9 was the solvent peak representing for the NaOH and NaAc. **c** The weight-average molecular weight of BEP, which was determined by HPLC (HPGPC, Agilent-1200, USA), and with a refractive index detector. **d** FT-IR spectrum of BEP in KBr. **e** UV spectra of BEP from 200 to 600 nm



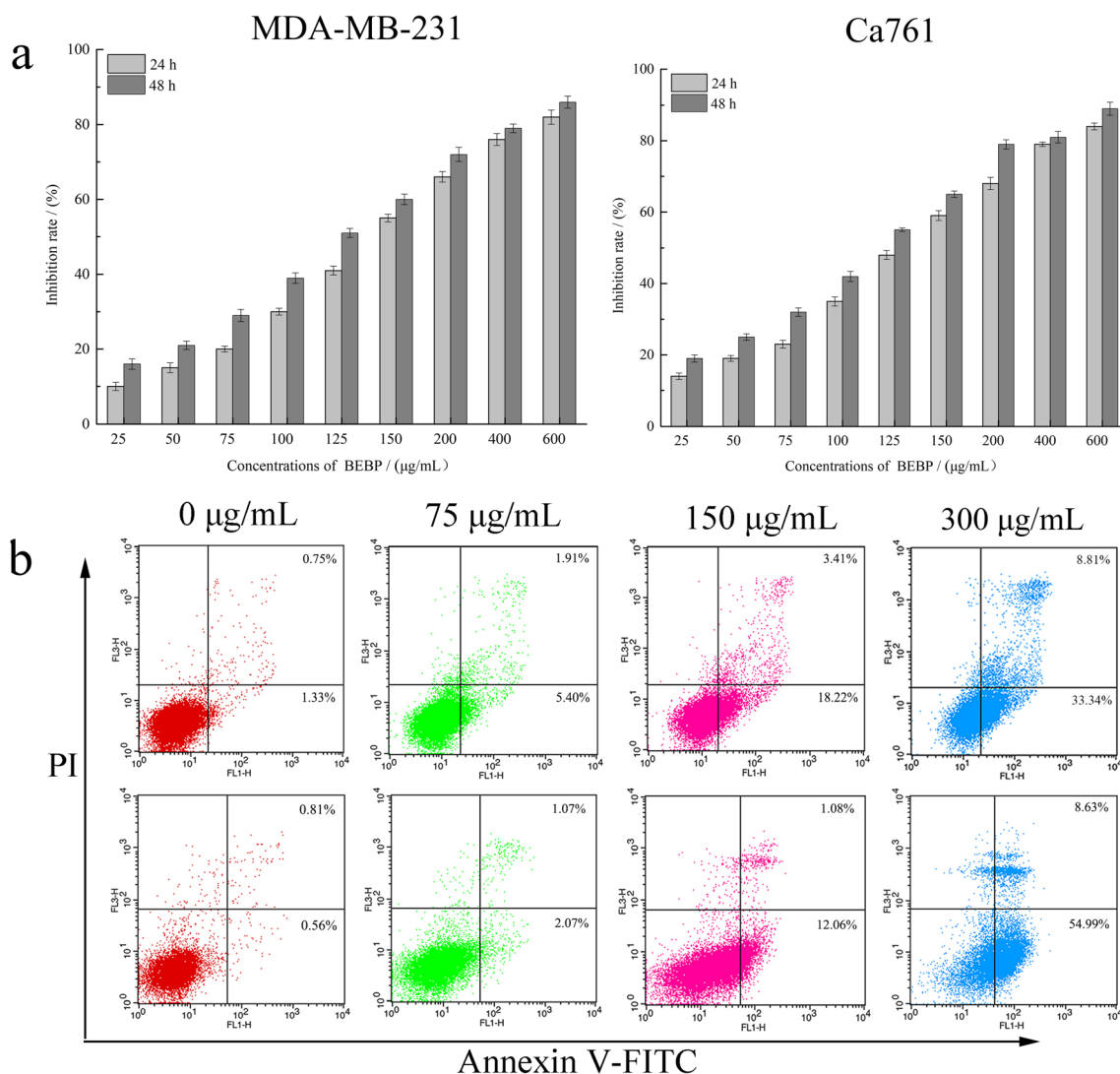


Fig. 2 **a** Inhibitory effect of BEP on MDA-MB-231 and Ca761 cells, respectively. **b** The apoptosis rates of MDA-MB-231 and Ca761 cells treated with BEP at different concentrations for 24 h and were detected

by flow cytometry after Annexin V-FITC/PI staining, $p < 0.05$ was considered statistically significant, compared with the control group

surface of the cell membrane began to shrink, and adherent-wall cells gradually decreased. As the concentration increases, the cells shrink severely and some break up into small particles.

As shown in Fig. 3b, e, the untreated breast cancer cells showed uniform pale blue fluorescence after staining with Hoechst 33258, indicating the nuclear morphology was complete. The blue fluorescence in the treated cells was gradually enhanced and showed lumpy bright blue fluorescence with the increase of BEP concentration, indicating that the chromatin of the nucleus was consolidated, which was consistent with the above morphological results.

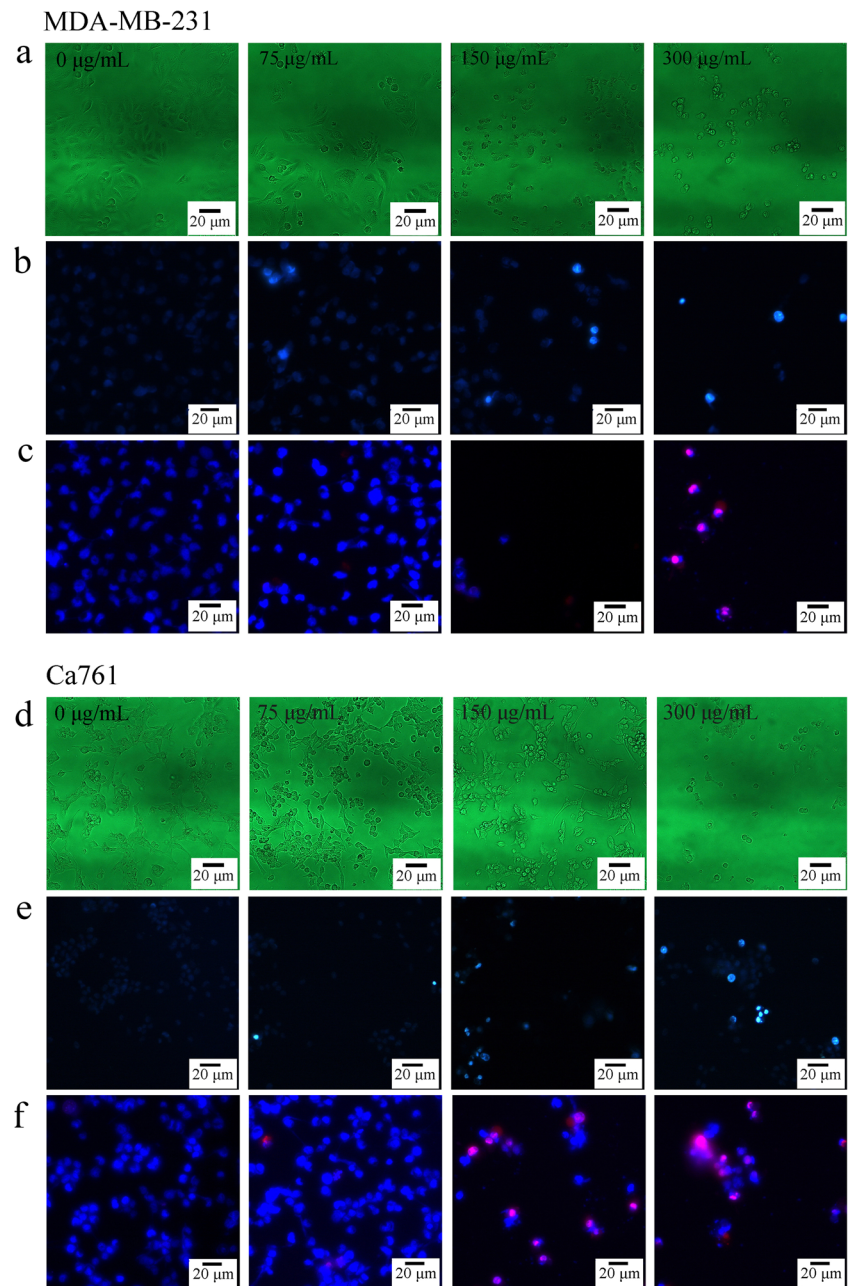
The morphological changes of apoptotic cells (Fig. 3c, f) were observed by Hoechst 33342/PI double staining under an inverted fluorescence microscope. The results showed that the untreated group of cells was stained weak blue by Hoechst

33342, whereas the low dose treatment groups present bright blue, suggesting they were in the early apoptosis state. With the increase of BEP concentration, most of the cells were stained bright blue, and part of the cells with pale purple, indicated that the cells were stained by Hoechst33342 and PI dyeing at the same time and in a state of late apoptosis. When the concentration of BEP was 300 µg/mL, some cells showed a fuchsia color, indicating that the membrane of the cells was broken and necrotic.

Cell apoptosis rate

The Annexin V-FITC/PI staining was used to detect the apoptosis rate. As shown in Fig. 2b, compared with the untreated groups, viable cells of the BEP-treated MDA-MB-231 and Ca761 cells were reduced, while apoptotic cells were

Fig. 3 Morphological changes of MDA-MB-231 and Ca761 cells were observed after BEBP treatment for 24 h. **a, d** Morphological changes were observed under a fluorescence inverted microscope ($\times 20$). **b, e** The changes of apoptotic nuclei after Hoechst 33258 staining were observed by a fluorescence inverted microscope ($\times 20$). **c, f** Hoechst 33324 and PI double staining was used to detect apoptotic cells by fluorescence inverted microscope ($\times 20$)



increased. With the concentration of BEP increased from 75 $\mu\text{g/mL}$ to 300 $\mu\text{g/mL}$, the apoptosis rate of MDA-MB-231 cells increased from 7.31% to 42.15% ($p < 0.05$), and Ca761 cells increased from 3.14% to 63.62% ($p < 0.05$), which suggested that Ca761 cells were more sensitive to BEP than MDA-MB-231 cells. The results showed that BEP could induce apoptosis and in a concentration-dependent manner.

Effect of BEP on the $\Delta\Psi_m$

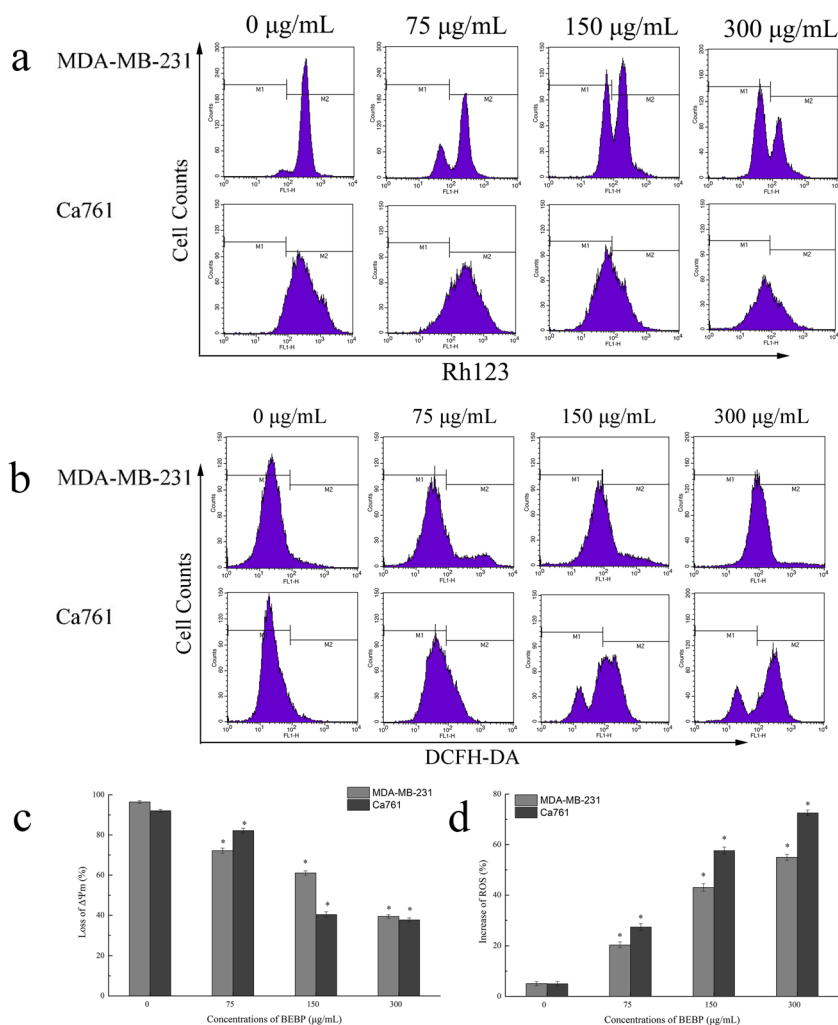
More and more evidence indicated that mitochondrial membrane potential collapse is a significant signal in the early

apoptosis [39, 40]. As shown in Fig. 4a, c, the positive cells significantly decreased from 96.37% to 39.43%, and 92% to 37.69% ($P < 0.05$), respectively. The results indicated that BEP induced the apoptosis of MDA-MB-231 and Ca761 cells in a concentration-dependent manner through the mitochondrial apoptosis pathway.

ROS generation analysis

With DCFH-DA as a fluorescent probe, the fluorescence intensity of cells at different periods was collected by flow cytometry to detect changes in intracellular ROS content. The results (Fig. 4b, d) showed that compared with the control

Fig. 4 **a** Histograms of the Rh 123-stained cells by flow cytometry. **b** Histograms of the DCFH-DA-stained cells by flow cytometry. **c** Columns represent the mitochondrial membrane potential changes. **d** Columns represent the ROS changes. Data are expressed as means \pm S.D. of three independent experiments. * $p < 0.05$, compared with control groups



group, the ROS content in MDA-MB-231 and Ca761 cells in the treated group was dose-dependence, from 5.03% to 54.96% and 4.99% to 72.58%, respectively, suggesting that BEP could induce apoptosis by increasing intracellular ROS damage.

BEP induced cell cycle arrest

The effects of BEP on the cell cycle of MDA-MB-231 and Ca761 cells were detected by PI staining. As shown in Fig. 5, the treated cells appeared sub-diploid peak (sub- G_1), which were getting bigger compared with the untreated cells, indicating that MDA-MB-231 and Ca761 cells were gradually apoptotic, which was consistent with Annexin V-FITC/PI double-staining results. Our results showed that with the increase of BEP concentration, the S-phase of MDA-MB-231 cells increased from 6.4% to 36.69%, and the G_0/G_1 phase of Ca761 cells increased from 26.01% to 72.24%, indicating that MDA-MB-231 and Ca761 cells were respectively blocked in the S-phase and G_0/G_1 phase.

Effect of BEP on the expressions of apoptosis-related proteins

To further confirm whether BEP induced apoptosis of breast cancer cells through the mitochondrial pathway, western blotting was used to detect the expression changes of apoptosis-related proteins in breast cancer cells after treatment with different concentrations of BEP. As shown in Fig. 6a, b, c, e, f, and g, the levels of cytochrome C in the cytosol were increased in a dose-dependence manner after BEP treatment compared with the control group. Also, the pro-apoptotic protein Bax was significantly increased, while anti-apoptotic protein Bcl-2 was significantly decreased, thereby increasing the Bax/Bcl-2 protein ratio ($p < 0.05$). Figure 6d, h showed that the cleaved-caspase-3 and cleaved-caspase-9 significantly increased compared to the control group in MDA-MB-231 and Ca761 cells treated with different concentrations of BEP. This suggested that the BEP induced apoptosis of MDA-MB-231 and Ca761 cells were activated by caspase-3 and caspase-9 proteins, which was dependent on the mitochondrial apoptosis pathway.

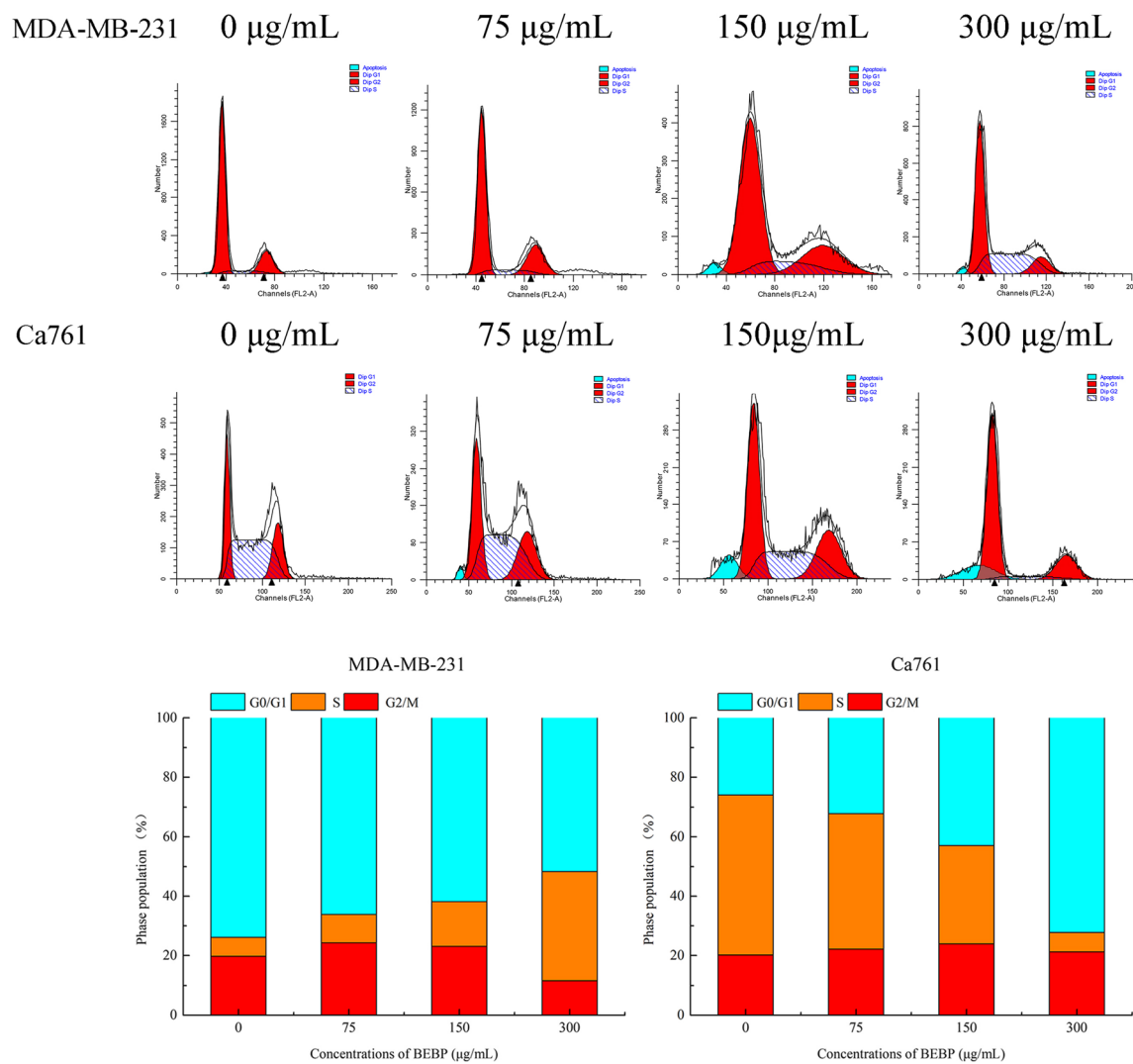


Fig. 5 The cell cycle distribution of MDA-MB-231 and Ca761 cells was changed after BEBP treatment with different concentrations for 24 h. Figures represent the distribution of different cell cycle phases. Bar graph of the cell population in G₀/G₁, S, and G₂/M phases

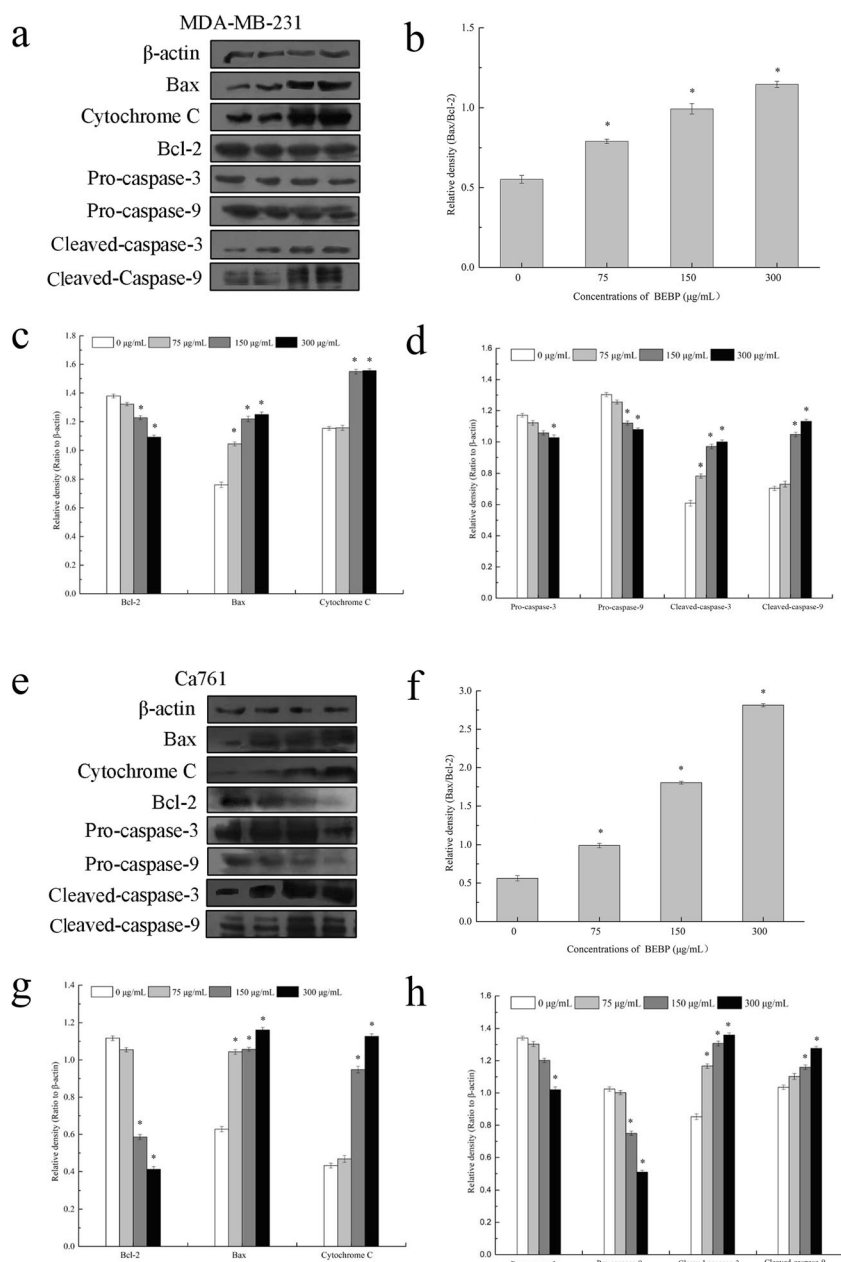
Discussion

With the increase of cancer morbidity and mortality, there were more and more cancer therapeutic methods, most of which were to induce apoptosis of cancer cells to achieve effective treatments, but which cause lots of unexpected toxic effects [41]. Polysaccharides extracted from natural sources are being used in clinical and therapeutic trials for patients, which exhibit include anti-oxidant, anti-cancer, anti-sclerotic, neuroprotective, anti-inflammatory, anti-allergic, antibacterial, antiviral, and hyperglycemic properties [9]. *Boletus edulis* is a kind of medicinal and food homologous fungus. Studies have shown that polysaccharides extracted from *Boletus edulis* had indirect antitumor activity achieved by improving the immune response [27]. However, its antitumor mechanism is still unclear.

In this study, we detected the cytotoxicity of BEP on MDA-MB-231 and Ca761 cells by MTT assay and found that

it inhibited the proliferation of both breast cancer cells in a dose-dependent manner, but Ca761 cells were more sensitive to BEP, which may be related to different cell types. After BEP treatment, the typical morphological features of apoptosis on MDA-MB-231 and Ca761 cells were observed under an inverted fluorescence microscope, including chromatin condensation, cytoplasmic concentration, cell membrane bubbles and the formation of apoptotic bodies. Besides, Honest 33,342/PI and Annexin V-FITC/PI staining showed that BEP could induce apoptosis (early apoptosis and late apoptosis) and even necrosis of these two breast cancer cells. Also, the absence of checkpoints leads to the dysregulation of the cell cycle could also lead to apoptosis [42]. By flow cytometry analysis, we found that BEP induced apoptosis of MDA-MB-231 and Ca761 cells by blocking them in the S phase and G₀/G₁ phase, respectively. These results indicated that BEP could induce apoptosis of MDA-MB-231 and Ca761 cells.

Fig. 6 **a, e** Western blotting analysis of Bax, Cytochrome c, Bcl-2, Pro-caspase-3, Pro-caspase-9, Cleaved-caspase-3, and Cleaved-caspase-9 expressions in MDA-MB-231 and Ca761 cells. **b, f** Quantitative analysis for a relative ratio of Bax to Bcl-2 in MDA-MB-231 and Ca761 cells. **c, g** Quantitative analysis for Bax, Bcl-2 and cytoplasmic cytochrome C levels normalized to β -actin in MDA-MB-231 and Ca761 cells. **d, h** Quantitative analysis for Pro-caspase-9/-3 and cleaved-caspase-9/-3 levels normalized to β -actin in MDA-MB-231 and Ca761 cells. Data were expressed as means \pm S.D. of three independent experiments. * $p < 0.05$, compared to untreated group



Apoptosis is a process of programmed cell death regulated by genes, which plays an important role in maintaining the stability of the intracellular environment, including the extrinsic death receptor pathway, mitochondrial pathway and endoplasmic reticulum pathway [43]. Mitochondrial apoptosis pathway is one of the classical apoptosis pathways [44]. The decreased mitochondrial membrane potential is an early marker of apoptosis in the mitochondrial apoptosis pathway, which may be related to the release of apoptotic factors, indicating the occurrence of apoptosis [45]. The Bcl-2 family proteins are the main regulatory factors of apoptosis, whereas caspases, a family of cysteine proteases, are the main executor of this process [46]. The Bcl-2 protein family includes pro-apoptotic and anti-apoptotic proteins, in which Bax can activate or inhibit Bcl-xl and Bad, while Bcl-2

can inhibit Bax [47]. Studies have shown that the ratio of Bax/Bcl-2 activity level, rather than the levels of individual proteins, is the key to apoptosis [48]. Reactive oxygen species (ROS) also play an important role in apoptosis and may inhibit cancer growth when endogenous oxidative stress levels are high [49]. Studies have shown that in the apoptosis of the intrinsic pathway, cytochrome C is released from mitochondria to cytoplasm, by targeting and activating caspase-9, thus leading to the activation of effector caspases-3 [50]. In our study, we found that BEP could increase of Bax/Bcl-2 ratio, promote the intracellular mitochondria permeability transition pore opening, significantly decrease the mitochondrial membrane potential, the release of cytochrome C, the elevation of ROS level, further activated caspase-9 and caspase-3, eventually lead to apoptosis.

Conclusion

In the present study, the polysaccharide (BEP) with a molecular weight of 6.0×10^6 Da were first extracted from *Boletus edulis*. IC indicated that BEP was an acid polysaccharide composed of galactose, glucose, xylose, mannose, glucuronic, and galacturonic acid (molar ratio: 0.34:0.28:0.28:2.57:1.00:0.44). We found that the polysaccharide (BEP) extracted in this study could inhibit the proliferation of MDA-MB-231 and Ca761 cells and induce them apoptosis through the mitochondrial pathway.

Acknowledgments Thanks to the College of Food Science and Engineering, Tianjin University of Science and Technology for supporting my research.

Compliance with ethical standards

Conflict of interest The authors declare that they have no conflicts of interest.

Ethical approval This article does not contain any studies with human participants or animals performed by any of the authors.

References

- Monnot, G.C., Romero, P.: Rationale for immunological approaches to breast cancer therapy. *Breast*. **37**, 187–195 (2018). <https://doi.org/10.1016/j.breast.2017.06.009>
- Wang, X., Yang, Y., An, Y., Fang, G.: The mechanism of anticancer action and potential clinical use of kaempferol in the treatment of breast cancer. *Biomed. Pharmacother.* **117**, 109086 (2019). <https://doi.org/10.1016/j.biopha.2019.109086>
- Goldhirsch, A., Winer, E.P., Coates, A.S., Gelber, R.D., Piccart-Gebhart, M., Thurlimann, B., Senn, H.J.: Personalizing the treatment of women with early breast cancer: highlights of the St Gallen International Expert Consensus on the Primary Therapy of Early Breast Cancer 2013. *Ann. Oncol.* **24**(9), 2206–2223 (2013). <https://doi.org/10.1093/annonc/mdt303>
- Bernier, J., Poortmans, P.M.: Surgery and radiation therapy of triple-negative breast cancers: from biology to clinics. *Breast*. **28**, 148–155 (2016). <https://doi.org/10.1016/j.breast.2016.05.014>
- Bauer, K.R., Brown, M., Cress, R.D., Parise, C.A., Caggiano, V.: Descriptive analysis of estrogen receptor (ER)-negative, progesterone receptor (PR)-negative, and HER2-negative invasive breast cancer, the so-called triple-negative phenotype: a population-based study from the California cancer registry. *Cancer*. **109**(9), 1721–1728 (2007). <https://doi.org/10.1002/cncr.22618>
- Meshkat, B., Prichard, R.S., Al-Hilli, Z., Bass, G.A., Quinn, C., O'Doherty, A., Rothwell, J., Geraghty, J., Evoy, D., McDermott, E.W.: A comparison of clinical-pathological characteristics between symptomatic and interval breast cancer. *Breast*. **24**(3), 278–282 (2015). <https://doi.org/10.1016/j.breast.2015.02.032>
- Moran, M.S., Yang, Q., Harris, L.N., Jones, B., Tuck, D.P., Haffty, B.G.: Long-term outcomes and clinicopathologic differences of African-American versus white patients treated with breast conservation therapy for early-stage breast cancer. *Cancer*. **113**(9), 2565–2574 (2008). <https://doi.org/10.1002/cncr.23881>
- Tajbakhsh, A., Rivandi, M., Abedini, S., Pasdar, A., Sahebkar, A.: Regulators and mechanisms of anoikis in triple-negative breast cancer (TNBC): a review. *Crit. Rev. Oncol. Hematol.* **140**, 17–27 (2019). <https://doi.org/10.1016/j.critrevonc.2019.05.009>
- Shamsaei, S., Getso, M., Ahmadikia, K., Yarahmadi, M., Farahani, H.E., Aslani, R., Mohammadzade, A.S., Raissi, V., Soleimani, A., Arghavan, B., Karami, S., Mohseni, M., Mohseni, M.S., Raiesi, O.: Recent findings on the role of fungal products in the treatment of cancer. *Clin. Transl. Oncol.* (2020). <https://doi.org/10.1007/s12094-020-02428-1>
- MacFarlane, M., Williams, A.C.: Apoptosis and disease: a life or death decision. *EMBO Rep.* **5**(7), 674–678 (2004). <https://doi.org/10.1038/sj.embor.7400191>
- Tang, X., Tang, J., Liu, X., Zeng, L., Cheng, C., Luo, Y., Li, L., Qin, S.L., Sang, Y., Deng, L.M., Lv, X.B.: Downregulation of miR-129-2 by promoter hypermethylation regulates breast cancer cell proliferation and apoptosis. *Oncol. Rep.* **35**(5), 2963–2969 (2016). <https://doi.org/10.3892/or.2016.4647>
- von Schwarzenberg, K., Vollmar, A.M.: Targeting apoptosis pathways by natural compounds in cancer: marine compounds as lead structures and chemical tools for cancer therapy. *Cancer Lett.* **332**(2), 295–303 (2013). <https://doi.org/10.1016/j.canlet.2010.07.004>
- Nicholson, D.W., Thornberry, N.A.: Caspases: killer proteases. *Trends Biochem. Sci.* **22**(8), 299–306 (1997). [https://doi.org/10.1016/S0968-0004\(97\)01085-2](https://doi.org/10.1016/S0968-0004(97)01085-2)
- Duprez, L., Wirawan, E., Vanden Berghe, T., Vandenabeele, P.: Major cell death pathways at a glance. *Microbes Infect.* **11**(13), 1050–1062 (2009). <https://doi.org/10.1016/j.micinf.2009.08.013>
- Levine, B., Sinha, S.C., Kroemer, G.J.A.: Bcl-2 family members: dual regulators of apoptosis and autophagy. *Autophagy*. **4**(5), 600–606 (2008). <https://doi.org/10.4161/auto.6260>
- Yan, X., Wang, L., Yang, X., Qiu, Y., Tian, X., Lv, Y., Tian, F., Song, G., Wang, T.: Fluoride induces apoptosis in H9c2 cardiomyocytes via the mitochondrial pathway. *Chemosphere*. **182**, 159–165 (2017). <https://doi.org/10.1016/j.chemosphere.2017.05.002>
- Cui, L., Bu, W., Song, J., Feng, L., Xu, T., Liu, D., Ding, W., Wang, J., Li, C., Ma, B., Luo, Y., Jiang, Z., Wang, C., Chen, J., Hou, J., Yan, H., Yang, L., Jia, X.: Apoptosis induction by alantolactone in breast cancer MDA-MB-231 cells through reactive oxygen species-mediated mitochondrion-dependent pathway. *Arch Pharm Res.* **41**(3), 299–313 (2018). <https://doi.org/10.1007/s12272-017-0990-2>
- Manzi, P., Gambelli, L., Marconi, S., Vivanti, V., Pizzoferrato, L.: Nutrients in edible mushrooms: an inter-species comparative study. *Food Chem.* **65**(4), 477–482 (1999). [https://doi.org/10.1016/S0308-8146\(98\)00212-X](https://doi.org/10.1016/S0308-8146(98)00212-X)
- Kalač, P.: Chemical composition and nutritional value of European species of wild growing mushrooms: a review. *Food Chem.* **113**(1), 9–16 (2009). <https://doi.org/10.1016/j.foodchem.2008.07.077>
- Ruthes, A.C., Smiderle, F.R., Iacomini, M.: d-Glucans from edible mushrooms: A review on the extraction, purification and chemical characterization approaches. *Carbohydr. Polym.* **117**, 753–761 (2015). <https://doi.org/10.1016/j.carbpol.2014.10.051>
- Zhang, H., Pu, D., Sun, B., Ren, F., Zhang, Y., Chen, H.: Characterization and comparison of key aroma compounds in raw and dry porcini mushroom (*Boletus edulis*) by aroma extract dilution analysis, quantitation and aroma recombination experiments. *Food Chem.* **258**, 260–268 (2018). <https://doi.org/10.1016/j.foodchem.2018.03.056>
- Dentinger, B.T., Ammirati, J.F., Both, E.E., Desjardin, D.E., Halling, R.E., Henkel, T.W., Moreau, P.A., Nagasawa, E., Soyong, K., Taylor, A.F., Watling, R., Moncalvo, J.M., McLaughlin, D.J.: Molecular phylogenetics of porcini mushrooms (*Boletus* section *Boletus*). *Mol. Phylogenet. Evol.* **57**(3), 1276–1292 (2010). <https://doi.org/10.1016/j.ympev.2010.10.004>

23. Chen, W., Wang, W.P., Zhang, H.S., Huang, Q.: Optimization of ultrasonic-assisted extraction of water-soluble polysaccharides from *Boletus edulis* mycelia using response surface methodology. *Carbohydr. Polym.* **87**(1), 614–619 (2012). <https://doi.org/10.1016/j.carbpol.2011.08.029>
24. Zhang, A.Q., Liu, Y., Xiao, N.N., Zhang, Y., Sun, P.L.: Structural investigation of a novel heteropolysaccharide from the fruiting bodies of *Boletus edulis*. *Food Chem.* **146**, 334–338 (2014). <https://doi.org/10.1016/j.foodchem.2013.09.073>
25. Zhang, A., Xiao, N., He, P., Sun, P.: Chemical analysis and antioxidant activity *in vitro* of polysaccharides extracted from *Boletus edulis*. *Int. J. Biol. Macromol.* **49**(5), 1092–1095 (2011). <https://doi.org/10.1016/j.ijbiomac.2011.09.005>
26. Lemieszek, M.K., Cardoso, C., Ferreira Milheiro Nunes, F.H., Ramos Novo Amorim de Barros, A.I., Marques, G., Pozarowski, P., Rzeski, W.: *Boletus edulis* biologically active biopolymers induce cell cycle arrest in human colon adenocarcinoma cells. *Food Funct.* **4**(4), 575–585 (2013). <https://doi.org/10.1039/c2fo30324h>
27. Wang, D., Sun, S.Q., Wu, W.Z., Yang, S.L., Tan, J.M.: Characterization of a water-soluble polysaccharide from *Boletus edulis* and its antitumor and immunomodulatory activities on renal cancer in mice. *Carbohydr. Polym.* **105**, 127–134 (2014). <https://doi.org/10.1016/j.carbpol.2013.12.085>
28. Zhang, L., Zhang, Q., Zheng, Y., He, Z., Guan, P., He, X., Hui, L., Dai, Y.: Study of Schiff base formation between dialdehyde cellulose and proteins, and its application for the deproteinization of crude polysaccharide extracts. *Ind. Crop. Prod.* **112**, 532–540 (2018). <https://doi.org/10.1016/j.indcrop.2017.12.056>
29. Dubois, M., Gilles, H.A., Hamilton, J.K., Rebers, P.A., Smith, F.: Colorimetric method for determination of sugars and related substances. *Anal. Chem.* **28**, 22–25 (1956). <https://doi.org/10.1021/ac60111a017>
30. Barbosa, H., Slater, N.K., Marcos, J.C.: Protein quantification in the presence of poly(ethylene glycol) and dextran using the Bradford method. *Anal. Biochem.* **395**(1), 108–110 (2009). <https://doi.org/10.1016/j.ab.2009.07.045>
31. Bitter, T., Muir, H.M.: A modified uronic acid carbazole reaction. *Anal. Biochem.* **4**(4), 330–334 (1962). [https://doi.org/10.1016/0003-2697\(62\)90095-7](https://doi.org/10.1016/0003-2697(62)90095-7)
32. Yu, J., Ji, H.Y., Liu, A.J.: Alcohol-soluble polysaccharide from *Astragalus membranaceus*: Preparation, characteristics and antitumor activity. *Int. J. Biol. Macromol.* **118**(Pt B), 2057–2064 (2018). <https://doi.org/10.1016/j.ijbiomac.2018.07.073>
33. Yu, J., Ji, H., Dong, X., Feng, Y., Liu, A.: Apoptosis of human gastric carcinoma MGC-803 cells induced by a novel *Astragalus membranaceus* polysaccharide via intrinsic mitochondrial pathways. *Int. J. Biol. Macromol.* **126**, 811–819 (2019). <https://doi.org/10.1016/j.ijbiomac.2018.12.268>
34. Yu, J., Ji, H., Yang, Z., Liu, A.: Relationship between structural properties and antitumor activity of *Astragalus* polysaccharides extracted with different temperatures. *Int. J. Biol. Macromol.* **124**, 469–477 (2019). <https://doi.org/10.1016/j.ijbiomac.2018.11.156>
35. Wang, Y., Li, Y., Liu, Y., Chen, X., Wei, X.: Extraction, characterization and antioxidant activities of se-enriched tea polysaccharides. *Int. J. Biol. Macromol.* **77**, 76–84 (2015). <https://doi.org/10.1016/j.ijbiomac.2015.02.052>
36. Zhao, Y., Liu, Y., Wang, W., Wu, D., Shi, J., Liu, A.: Apoptosis and autophagy induction of Seleno- β -lactoglobulin (Se- β -Lg) on hepatocellular carcinoma cells lines. *J. Funct. Foods* **49**, 412–423 (2018). <https://doi.org/10.1016/j.jff.2018.09.011>
37. Zhang, L., Li, X., Deng, H., Jing, Y., Fu, Q.: Enhanced thermal conductivity and electrical insulation properties of polymer composites via constructing Pglass/CNTs confined hybrid fillers. *Compos. A: Appl. Sci. Manuf.* **115**, 1–7 (2018). <https://doi.org/10.1016/j.compositesa.2018.09.009>
38. Kong, L., Yu, L., Feng, T., Yin, X., Liu, T., Dong, L.: Physicochemical characterization of the polysaccharide from *Bletilla striata*: effect of drying method. *Carbohydr. Polym.* **125**, 1–8 (2015). <https://doi.org/10.1016/j.carbpol.2015.02.042>
39. Jose, G.M., Raghavankutty, M., Kurup, G.M.: Sulfated polysaccharides from *Padina tetrastratica* induce apoptosis in HeLa cells through ROS triggered mitochondrial pathway. *Process Biochem.* **68**, 197–204 (2018). <https://doi.org/10.1016/j.procbio.2018.02.014>
40. Chen, D., Sun, S., Cai, D., Kong, G.: Induction of mitochondrial-dependent apoptosis in T24 cells by a selenium (Se)-containing polysaccharide from *Ginkgo biloba* L. leaves. *Int. J. Biol. Macromol.* **101**, 126–130 (2017). <https://doi.org/10.1016/j.ijbiomac.2017.03.033>
41. Cui, H., Wang, C., Wang, Y., Li, Z., Zhang, Y., Chen, M., Li, F.: *Pleurotus nebrodensis* polysaccharide induces apoptosis in human non-small cell lung cancer A549 cells. *Carbohydr. Polym.* **104**, 246–252 (2014). <https://doi.org/10.1016/j.carbpol.2014.01.001>
42. Azzopardi, M., Farrugia, G., Balzan, R.: Cell-cycle involvement in autophagy and apoptosis in yeast. *Mech. Ageing Dev.* **161**(Pt B), 211–224 (2017). <https://doi.org/10.1016/j.mad.2016.07.006>
43. Wang, Y., Huo, T., Feng, C., Zeng, Y., Yang, J., Zhang, X., Dong, F., Deng, J.: Chrysotile asbestos induces apoptosis via activation of the p53-regulated mitochondrial pathway mediated by ROS in A549 cells. *Appl. Clay Sci.* **182**, 105245 (2019). <https://doi.org/10.1016/j.clay.2019.105245>
44. Chen, G., Zhang, P., Huang, T., Yu, W., Lin, J., Li, P., Chen, K.: Polysaccharides from *Rhizopus nigricans* mycelia induced apoptosis and G2/M arrest in BGC-823 cells. *Carbohydr. Polym.* **97**(2), 800–808 (2013). <https://doi.org/10.1016/j.carbpol.2013.05.068>
45. Wang, A., Si, Z., Xue, P., Li, X., Liu, J.: Tacrolimus protects hippocampal neurons of rats with status epilepticus through suppressing oxidative stress and inhibiting mitochondrial pathway of apoptosis. *Brain Res.* **1715**, 176–181 (2019). <https://doi.org/10.1016/j.brainres.2019.02.031>
46. Gross, A.: BCL-2 family proteins as regulators of mitochondria metabolism. *Biochim. Biophys. Acta* **1857**(8), 1243–1246 (2016). <https://doi.org/10.1016/j.bbabi.2016.01.017>
47. Du, L., Fei, Z., Song, S., Wei, N.: Antitumor activity of Lobaplatin against esophageal squamous cell carcinoma through caspase-dependent apoptosis and increasing the Bax/Bcl-2 ratio. *Biomed. Pharmacother.* **95**, 447–452 (2017). <https://doi.org/10.1016/j.biopha.2017.08.119>
48. Vucicevic, K., Jakovljevic, V., Colovic, N., Tosic, N., Kostic, T., Glumac, I., Pavlovic, S., Karan-Djurasevic, T., Colovic, M.: Association of Bax expression and Bcl2/Bax ratio with clinical and molecular prognostic markers in chronic lymphocytic leukemia. *J. Med. Biochem.* **35**(2), 150–157 (2016). <https://doi.org/10.1515/jomb-2015-0017>
49. Yao, W., Lin, Z., Shi, P., Chen, B., Wang, G., Huang, J., Sui, Y., Liu, Q., Li, S., Lin, X., Yao, H.: Delicaflavone induces ROS-mediated apoptosis and inhibits PI3K/AKT/mTOR and Ras/MEK/Erk signaling pathways in colorectal cancer cells. *Biochem. Pharmacol.* **171**, 113680 (2019). <https://doi.org/10.1016/j.bcp.2019.113680>
50. Zhong, Y., Jin, C., Gan, J., Wang, X., Shi, Z., Xia, X., Peng, X.: Apigenin attenuates patulin-induced apoptosis in HEK293 cells by modulating ROS-mediated mitochondrial dysfunction and caspase signal pathway. *Toxicol.* **137**, 106–113 (2017). <https://doi.org/10.1016/j.toxicol.2017.07.018>

Publisher's note Springer Nature remains neutral with regard to jurisdictional claims in published maps and institutional affiliations.